RSC Pharmaceutics

ROYAL SOCIETY OF CHEMISTRY

PAPER

View Article Online
View Journal

Cite this: DOI: 10.1039/d5pm00258c

A simple and cost-effective chrysin–theophylline eutectic: enhanced solubility, dissolution, and oral bioavailability with potential for respiratory applications

Sanket Sirmanwar and Sharvil Patil *

Asthma and chronic obstructive pulmonary disease (COPD) are the most prevalent chronic respiratory diseases. Theophylline is used for its bronchodilator and anti-inflammatory effects, but its clinical use is declining due to its narrow therapeutic index and metabolism by cytochrome enzymes, which increases the risk of drug interactions and toxicity. Chrysin, a BCS class II flavonoid, exhibits anti-inflammatory and antioxidant activities and is reported to inhibit cytochrome enzymes. Drug–drug eutectic mixtures are increasingly explored to enhance the solubility and bioavailability of poorly water-soluble drugs. In this context, a eutectic mixture of chrysin and theophylline was prepared using a simple, eco-friendly grinding method, with theophylline (a BCS class I drug) serving as a coformer. The prepared eutectic was characterized by differential scanning calorimetry (DSC), Fourier transform infrared spectroscopy (FTIR), hot stage microscopy (HSM), powder X-ray diffraction (PXRD), thermogravimetric analysis (TGA), scanning electron microscopy with energy dispersive spectroscopy (FE SEM-EDS), *in vitro* dissolution studies and *in vivo* pharmacokinetic evaluation in Wistar rats. DSC studies confirmed eutectic formation as its melting point was below those of chrysin and theophylline. They also confirmed a stoichiometric ratio of 1 : 2 between chrysin and theophylline. FTIR studies suggested intermolecular hydrogen bonding between chrysin and theophylline. The eutectic mixture significantly improved the aqueous solubility and dissolution rate of chrysin. Pharmacokinetic studies in rats showed a 3-fold increase in area under the curve (AUC) and a 2.87-fold increase in relative bioavailability of chrysin. This dual-drug eutectic may offer combined anti-inflammatory benefits and improved bioavailability for both agents, with chrysin's cytochrome inhibition potentially reducing theophylline degradation, supporting its therapeutic potential for possible use in asthma and COPD.

Received 22nd September 2025,
Accepted 8th January 2026

DOI: 10.1039/d5pm00258c

rsc.li/RSCPharma

1. Introduction

Asthma and Chronic Obstructive Pulmonary Disease (COPD) are the two most common chronic respiratory illnesses in the world that present a substantial and increasing public health burden. Globally, COPD is a major contributor to illness and death. According to the Global Burden of Disease (GBD) study, there were around 212.3 million cases of COPD in 2019. 3.3 million people died around the world. Additionally, according to data from the World Health Organization (WHO), 262 million individuals suffered from asthma in 2019, resulting in 455 000 fatalities.[1,2] Theophylline (THEO), a methylxanthine, is the most commonly used drug for the treatment of asthma and COPD due to its dual bronchodilator and anti-inflammatory actions. THEO displays its bronchodilator action through inhibition of phosphodiesterase, ultimately increasing cAMP and anti-inflammatory action by curbing inflammatory pathways such as NF-κB and PI3K/Akt.[3,4] However, though cost-effective, the use of THEO is declining due to its narrow therapeutic index and metabolism by cytochrome enzymes (CYP1A2).[5]The combination of drugs could improve the beneficial therapeutic effects of THEO.

Chrysin (CHRY) is a 5,7-dihydroxyflavone molecule obtained from herbs such as *Passiflora caerulea* and *Passiflora incarnata* and propolis. CHRY exhibits potential anti-inflammatory activity through inhibition of NF-κB and reduction in cytokines, and antioxidant activity by scavenging free radicals.[6,7] Furthermore, CHRY has shown inhibitory effects on CYP1A2 enzymes.[8] Thus, the combination of THEO and CHRY could offer synergistic benefits, enhancing anti-inflammatory and antioxidant protection while potentially reducing

Department of Pharmaceutics, Poona College of Pharmacy, Bharati Vidyapeeth (Deemed to be University), Pune, Maharashtra, India.
E-mail: sharvilpatil25@gmail.com, sharvil.patil@bharatividyapeeth.edu;
Fax: +91 20 25439383; Tel: +91 20 25437237

the required dose and toxicity risk of THEO. However, CHRY belongs to BCS class II, having poor aqueous solubility and in turn bioavailability, while THEO belongs to BCS class I,[8] which poses a hurdle in the combination of these two molecules.

Crystal engineering is one of the widely used approaches to resolve the poor solubility issues of drug molecules. Furthermore, drug–drug cocrystals or eutectic formulations could be helpful in combining two molecules for mutual pharmacological benefits and also altering the physicochemical properties of the drug molecules. Eutectic mixtures have gained popularity for altering the physicochemical properties of drug molecules due to their simple and cost-effective preparation methods. A eutectic mixture, mostly a two-component system, includes a drug often belonging to BCS class II/IV and a water-soluble coformer combined in a specific molar ratio, exhibiting a single melting point that is lower than the melting points of the individual components. Eutectic mixtures have shown enhanced aqueous solubility, bioavailability and/or stability of poorly water soluble drugs.[9–11]

Thus, in the present work, a drug–drug eutectic of CHRY and THEO has been attempted, wherein THEO is used as a coformer. The prepared eutectic was characterized using differential scanning calorimetry (DSC), Fourier transform infrared spectroscopy (FTIR), powder X-ray diffraction (PXRD), hot stage microscopy (HSM), thermogravimetric analysis (TGA) and energy dispersive spectroscopy (EDS). Furthermore, saturation solubility studies, *in vitro* dissolution studies using USP type IV apparatus and *in vivo* pharmacokinetic studies in male Wistar rats were carried out for the prepared eutectic mixture.

2. Materials and methods

2.1 Materials

Chrysin (CHRY), a light yellow crystalline solid powder, with >98% purity was purchased from Tokyo Chemical Industry, Japan, and anhydrous theophylline (THEO) with >98.5% purity to be used as a co-former was purchased from Sisco Research Laboratories (SRL) Pvt Ltd, India. Methanol was purchased from MSB Chemical Ltd, India. Milli-Q water was obtained from a Milli-Q water purification assembly.

2.2 Preparation of the eutectic mixture

The eutectic mixture of CHRY was prepared using the dry grinding method. CHRY (0.1 mmol) and theophylline (0.1 mmol and 0.2 mmol) were weighed accurately and mixed thoroughly in 1 : 1 and 1 : 2 stoichiometric ratios using a glass mortar and pestle under ambient conditions without the addition of any solvent for 2–3 minutes. The mixture thus obtained was characterized further.

2.3 Characterization of the eutectic mixture

2.3.1 Differential scanning calorimetry (DSC) analysis. The DSC thermograms of CHRY, THEO, and CHRY–THEO (1 : 1) and CHRY–THEO (1 : 2) eutectic mixtures were recorded using a differential scanning calorimeter (DSC7020 model, Hitachi, Japan). The samples (3–5 mg) were hermetically sealed in an aluminum pan and heated in a temperature range of 0–300 °C at a rate of 10 °C min^{-1} in a continuous nitrogen purging environment.

2.3.2 Hot stage microscopy studies (HSM). A Linkam Scientific Instrument Ltd (Tadworth, England) instrument outfitted with an EHEIM professional 4+ temperature controller and an optical microscope (Leica S8AP0) equipped with a Q imaging camera was used to perform hot stage microscopy of the eutectic mixture. The sample CHRY–THEO (1 : 2) was heated from 50 to 250 °C at a rate of 10 °C min^{-1} in order to determine the melting point. The sample was brought into focus under the microscope at 10× magnification, and images were captured at predetermined time intervals during the heating process.

2.3.3 Fourier transform infrared spectroscopy (FTIR). The FTIR spectra of CHRY, THEO, and CHRY–THEO (1 : 2) were recorded using a Fourier transform infrared spectrophotometer (FTIR 8400, Jaco, Tokyo, Japan). The samples were triturated individually with KBr in a 1 : 9 ratio and filled in IR slots to scan them in the range of 3600 to 600 cm^{-1}. The spectra were analysed using Spectra Manager software (JASCO). A blank KBr spectrum was also run to minimize interference of peaks.

2.3.4 Powder X-ray diffraction (PXRD). The PXRD patterns of CHRY and CHRY : THEO (1 : 2) were recorded using an X-ray diffractometer (Xpert PRO diffractometer, PANalytical, Almelo, The Netherlands). The diffractometer used Cu-Kα radiation to produce a precise X-ray powder diffraction pattern, and the voltage and current of the tube were set at 45 kV and 40 mA, respectively. The divergence and anti-scattering slits were set at 0.48° for the diffraction experiment with a sample size of 10 mm. Each sample was kept in a glass sample container and scanned in the 2θ range of 3.5° and 50° with a step size of 0.017° and a step length of 25 seconds per step. Malvern Panalytical's X'Pert HighScore software was used to enhance the experimental PXRD patterns.

2.3.5 Thermogravimetric analysis. TGA of CHRY and CHRY–THEO (1 : 2) was performed using a PerkinElmer STA 6000 Simultaneous Thermal Analyzer (Waltham, MA, USA). The alumina crucible containing 5–10 mg of CHRY and CHRY–THEO (1 : 2) powder was heated individually in the temperature range of 25–600 °C at a rate of 10 °C per minute. Dry nitrogen was continuously purged at a rate of 50 mL min^{-1} to maintain an inert atmosphere throughout the analysis. The weight loss of the sample was analysed using Pyris Manager software.

2.3.6 Field emission scanning electron microscopy (FE-SEM)-energy dispersive spectroscopy (EDS). The FE-SEM images of CHRY and CHRY–THEO (1 : 2) were recorded using an FEI Nova NanoSEM 450 fitted with a Bruker XFlash 6I30 EDS (Billerica, Massachusetts, USA). Each sample, *viz*. CHRY and CHRY–THEO (1 : 2), was placed on carbon tape and sputter-coated before mounting on a stub to record the photomicrograph and EDS pattern. Energy dispersive X-ray spec-

troscopy is powerful technique used to identify the elemental composition of a sample, particularly electronegative atoms such as oxygen (O), nitrogen (N), and the OH group that participate in the hydrogen bonding process. Furthermore, the particle morphologies of CHRY and CHRY–THEO (1 : 2) in terms of circularity, convexity, solidity, intensity, texture, HS circularity, sphericity, and elongation were recorded using a BX53 Olympus microscope. The data analysis was performed using CLAIRITY™ (particle size analysis software).

2.3.7 Saturation solubility study. The saturation solubility of CHRY and the prepared CHRY–THEO (1 : 2) was recorded. CHRY and CHRY–THEO samples were placed in excess in glass vials filled with water, 0.1 N HCl, and phosphate buffer (pH 6.8, 10 mL) and kept on a rotary shaker for 24 h at 37 °C before analysis. The samples were filtered using a Millipore nylon membrane filter (0.45 μm) to remove any undissolved CHRY. The filtrates were scanned using a UV visible spectrophotometer (JASCO, Tokyo, Japan) at 270 nm.

2.3.8 *In vitro* dissolution study. Flow through cell apparatus (USP Type IV, Sotax India Pvt Ltd, India) was used to perform *in vitro* dissolution tests for CHRY and CHRY–THEO (1 : 2). A cell of an internal diameter of 12 mm was used for the *in vitro* dissolution study. The fluid jet entering the cell was equalized by placing a 5 mm ruby bead at the apex of the bottom cone. The amount of sample loaded in the cell was equivalent to 10 mg of CHRY and CHRY–THEO individually after passing through 60-mesh sieves (mesh size 250 μm). To retain undissolved particles, a Whatman® glass fibre filter (GF/F, 0.7 μm pore size) was placed on the upper section of the cell.[12] The dissolution medium (phosphate buffer pH 6.8) was pumped (120 pulses per minute) through the cell and the test was performed at 37 ± 0.5 °C with a flow rate of 16 mL min^{-1} for 6 h followed by a change in the dissolution medium to phosphate buffer pH 6.8. The dissolution test was performed under non-sink conditions with a media volume of 250 mL. The aliquots were collected at 5, 10, 15, 30, 45, 60, 90, 120, 180, 240, 300 and 360 min. The CHRY concentration was determined using a UV visible spectrophotometer by recording the absorbance at 268 nm.

2.3.9 *In vivo* pharmacokinetic study. The pharmacokinetic parameters of CHRY and CHRY–THEO (1 : 2) samples upon oral administration to rats were recorded. Male Wistar rats weighing between 230 and 250 grams were used for the study. The animal experimental protocol received approval from the Institutional Animal Ethics Committee (IAEC) of Poona College of Pharmacy, Pune, India, under reference number PCP/IAEC/2025/1-23. The animals were kept in an environmentally controlled area with free access to food and water. The animals were divided into two groups, each containing 6 animals. The first group received a single oral dose equivalent to 10 mg per kg body weight of an aqueous dispersion of CHRY alone while the other group received a solution of CHRY–THEO (1 : 2) using an oral gavage syringe in the fasting state. The animals were anesthetized using ether for each sample and blood was taken at regular intervals by puncturing the retro-orbital plexus (ROP). Blood samples (1 ml) were collected from the retro-orbital plexus at 15, 30, 60, 120, 240, 360, 480, 720, and 1440 minutes. The samples were centrifuged at 8000 rpm for 20 minutes at 4 °C to separate the plasma. The supernatant was stored at −20 °C before analysis. The plasma concentration of CHRY was determined using the HPLC method. The pharmacokinetic parameters such as C_{max}, T_{max} and $AUC_{0-\infty}$ were estimated from the plasma CHRY concentration *versus* time profile using PK Solver Pk2 software.

HPLC method. A HPLC system (PU 2080, Japan) fitted with a Hypersil C_{18} column with specifications of 5 μm, 250 mm × 4.6 mm was used to determine the concentration of CHRY. The mobile phase consisted of methanol and water in an 85 : 15 v/v ratio. The mobile phase underwent filtration with a 0.45 μm Millipore filter and was degassed before use. The detector was tuned to a wavelength of 268 nm, with the flow rate regulated at 1 ml min^{-1}. The ratio of the chromatographic peak area of CHRY to that of the internal standard (cinnamic acid) was used for quantitative analysis.[7] The internal standard was prepared at a concentration of 1 μg ml^{-1}. CHRY concentrations ranging from 0.2 to 10 μg ml^{-1} exhibited a strong linear relationship with an R^2 value of 0.9989.

HPLC analysis of CHRY in plasma. Known concentrations of CHRY (0.5–10 μg ml^{-1}) and the internal standard (1 μg ml^{-1}) were premixed with plasma, and methanol was used as the extraction solvent. A blank sample was prepared using unspiked plasma. After vortexing for 1 minute, the mixture was centrifuged at 4 °C at a speed of 8000 rpm. The resulting supernatant was collected and introduced into the HPLC system.

3. Results and discussion

Several common methods for the preparation of eutectic mixtures have been reported, such as simple mixing, heating and stirring, ultrasound/microwave assisted synthesis and mechanical grinding.[13,14] Considering the potential advantages such as solvent free process, low cost, improved solid state interactions due to application of mechanical energy, faster processing time, scalability and devoid of the possibility of polymorphic transformation or solvent inclusion of the dry grinding method, it was utilized for the preparation of the eutectic mixture.

3.1 Differential scanning calorimetry (DSC) analysis

Initially, CHRY was mixed with THEO in a stoichiometric ratio of 1 : 1 and 1 : 2. DSC studies were performed to ascertain the exact stoichiometric ratio of CHRY and THEO. The DSC thermograms of CHRY and THEO showed a sharp endothermic peak at 289.5 °C with a melting enthalpy of 123 mJ mg^{-1} and at 274.6 °C with an enthalpy of 132 mJ mg^{-1}, respectively, indicating their crystalline nature (Fig. 1). Surprisingly, the DSC thermogram of CHRY : THEO (1 : 1) showed two peaks, one at 227.3 °C and the other at 286.2 °C. It is well reported in the literature that the melting point of a eutectic mixture is below the melting points of the individual components.[15–17] In the case of CHRY : THEO (1 : 1), the first endothermic peak

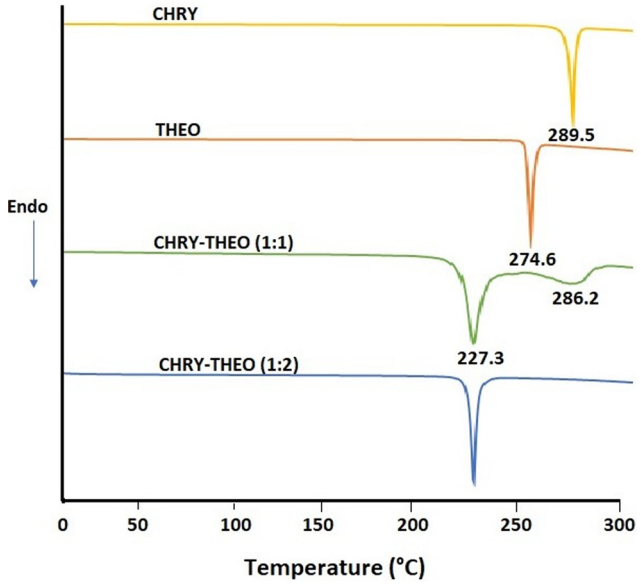

Fig. 1 DSC thermograms of CHRY, THEO, CHRY–THEO (1 : 1) and CHRY–THEO (1 : 2).

observed at 227.3 °C suggested the possibility of the formation of a eutectic mixture; however, the broad endothermic peak observed at 286.2 °C was indicative of melting of unreacted CHRY. Thus, DSC studies suggested incomplete formation of a eutectic mixture at a 1 : 1 stoichiometric ratio of CHRY and THEO. Therefore, it was decided to increase the amount of the coformer (THEO) and record the DSC thermogram of CHRY–THEO at a 1 : 2 stoichiometric ratio. The DSC thermogram of CHRY–THEO (1 : 2) showed a single melting endotherm at 227.3 °C with a melting enthalpy of 116 mJ mg^{-1}, which is lower than those of both pure chrysin and pure theophylline, confirming the formation of a eutectic mixture. Furthermore, DSC studies also ascertained the exact stoichiometric ratio for CHRY and THEO respectively.

3.2 Hot stage microscopy

HSM of the prepared CHRY–THEO (1 : 2) eutectic mixture was performed to validate the readings of DSC (Fig. 2). The HSM study showed complete melting of the eutectic mixture near 230 °C, leaving no residue of CHRY or THEO. The mixture displayed sharp melting as visible in the HSM photographs, suggesting depression of the melting point of the individual components, *i.e.* CHRY and THEO. Moreover, no crystallization was recorded upon cooling the molten mixture. Thus, the findings of the HSM study were in agreement with DSC. The reduction in the melting point of the eutectic mixture as compared to the individual components is attributed to the enhanced entropy of mixing and strong intermolecular interactions such as hydrogen bonding that disrupts the crystal lattices of the pure components.[2,12,17–20]

3.3 FTIR

FTIR can be used to determine the chemical interactions among the drug and the coformer. The FTIR spectra of CHRY, THEO and the CHRY–THEO (1 : 2) eutectic mixture are depicted in Fig. 3. The FTIR spectrum of CHRY showed characteristic absorption peaks at 1605 cm^{-1} associated with aromatic C=C stretching and aromatic ring vibrations, at 1639 cm^{-1} associated with C=O stretching of the flavone carbonyl group, and at 3410 cm^{-1} and 3230 cm^{-1} attributed to the phenolic hydroxyl groups associated with C-5 and C-7 (ref. 21 and 22) (Table 1). The FTIR spectrum of THEO showed characteristic absorption peaks at 3000 cm^{-1} associated with

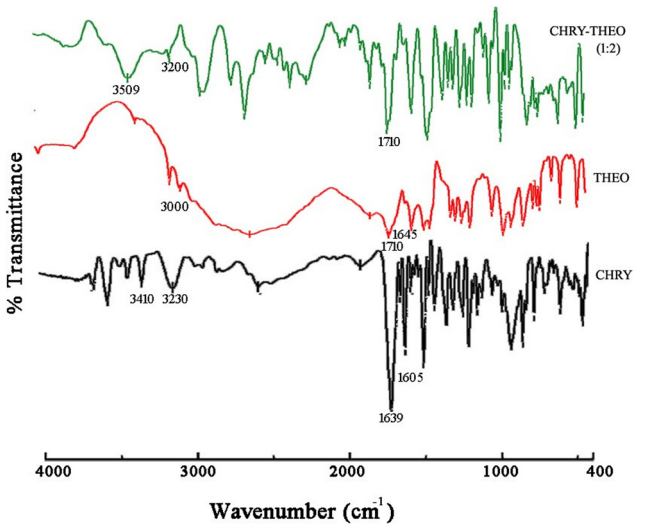

Fig. 3 Fourier transform infrared spectra of CHRY, THEO and CHRY–THEO (1 : 2).

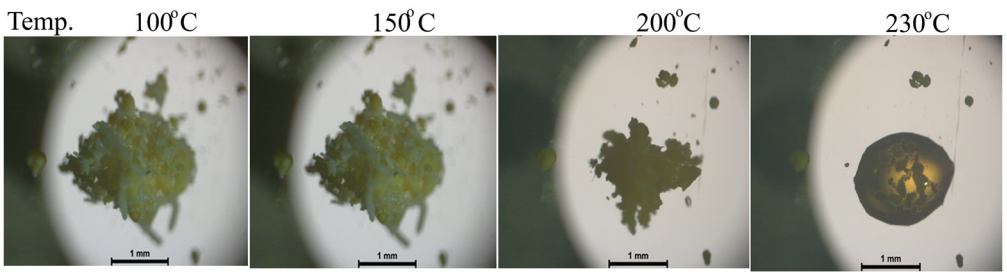

Fig. 2 Hot stage microscopy images of CHRY–THEO (1 : 2) at different temperatures.

Table 1 FTIR absorption peaks of chrysin, theophylline and the chrysin : theophylline (1 : 2) eutectic mixture

Sr. no.	Sample	FTIR peaks (% transmittance)
1	CHRY	1605 cm^{-1} (aromatic C=C stretching and aromatic ring vibrations), 1639 cm^{-1} (C=O stretching of the flavone carbonyl group), 3410 cm^{-1} and 3230 cm^{-1} (phenolic hydroxyl groups associated with C-5 and C-7)
2	THEO	3000 cm^{-1} [N–H stretching (N-9)], 1710 cm^{-1} (carbonyl C=O stretching at C-2), 1645 cm^{-1} (secondary amine stretching)
3	CHRY–THEO (1 : 2)	3509 cm^{-1} and 3200 cm^{-1} for the O–H groups of CHRY associated with C-5 and C-7, 1710 cm^{-1} corresponding to C=O stretching (C-2) of THEO

N–H stretching (N-9), at 1710 cm^{-1} associated with carbonyl C=O stretching at C-2, and at 1645 cm^{-1} associated with secondary amine stretching.[23,24] The FTIR spectra of CHRY : THEO (1 : 2) showed a broad peak with a red shift at 3509 cm^{-1} and a blue shift at 3200 cm^{-1} for the O–H groups of CHRY associated with C-5 and C-7, with the absence of a peak at 3000 cm^{-1} associated with N–H stretching of THEO, along with the retention of the absorption peak at 1710 cm^{-1} corresponding to C=O stretching (C-2) of THEO (Fig. 4). Thus, FTIR studies suggested hydrogen bond interactions between the O–H groups of CHRY and the N–H group of THEO and also justified the stoichiometric ratio of CHRY and THEO as 1 : 2.

3.4 Powder X-ray diffraction (PXRD)

The PXRD patterns of CHRY and CHRY–THEO (1 : 2) are presented in Fig. 5. PXRD can be used to predict the formation of a new crystal phase if there is a change in the PXRD pattern of the drug and/or coformer. The PXRD pattern of CHRY showed characteristic sharp diffraction peaks at 7.37°, 12.61°, 14.91°, 17.82°, 25.24° and 28.23° 2θ.[25] Similarly, the PXRD pattern of THEO displayed characteristic sharp diffraction peaks at 7.14°, 12.62°, 14.46°, 23.7°, 24.26°, 25.94°, 26.74°, 27.68°, and 29.68° 2θ.[26] The PXRD pattern of the CHRY–THEO (1 : 2) eutectic mixture displayed diffraction peaks at 7.6°, 12.7°, 14.02°, 17.54°, 26.42°, 27.62°, 28.54°, and 30.18°, suggesting mere addition of peaks with minute changes. Thus, the PXRD findings supported the readings of DSC, suggesting the formation of a eutectic mixture as no new peaks were observed in PXRD.

3.5 Thermogravimetric analysis

TGA was performed to assess the thermal stability of the prepared eutectic mixture.[27,28] Fig. 6 depicts the TGA graphs of CHRY and the CHRY–THEO (1 : 2) eutectic mixture. The TGA graph of CHRY did not show any weight loss at lower temperatures, although its degradation initiated at 285 °C. Similarly, the TGA graph of the CHRY–THEO (1 : 2) eutectic mixture also showed a single weight loss due to the degradation initiated at 230 °C. Thus, the TGA studies confirmed the thermal stability of the prepared eutectic mixture.

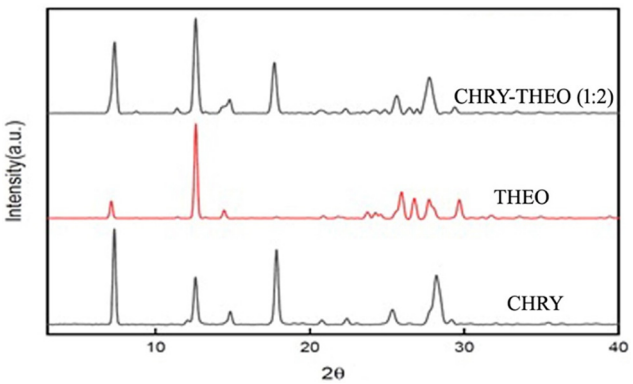

Fig. 5 PXRD patterns of CHRY, THEO and the CHRY–THEO (1 : 2) eutectic mixture.

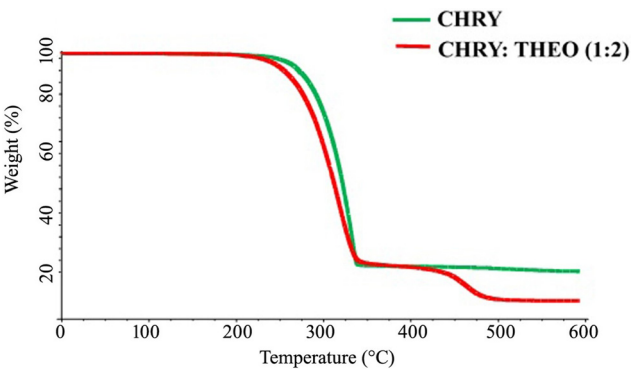

Fig. 6 TGA curves of CHRY and the CHRY–THEO (1 : 2) eutectic mixture.

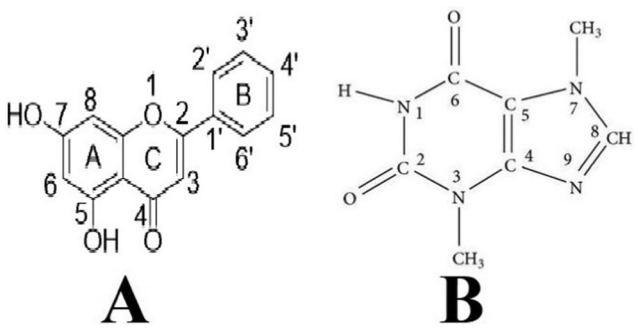

Fig. 4 Chemical structures of (A) CHRY and (B) THEO.

3.6 FE-SEM-EDS

Energy dispersive X-ray spectroscopy (EDS), typically coupled with scanning electron microscopy (SEM), is a technique used for surface elemental analysis. EDS cannot directly detect hydrogen because of its low atomic number; however, it can confirm the presence of atoms such as F, N, and O[27,28] for ascertaining the purity of the sample. Fig. 7 presents the EDS

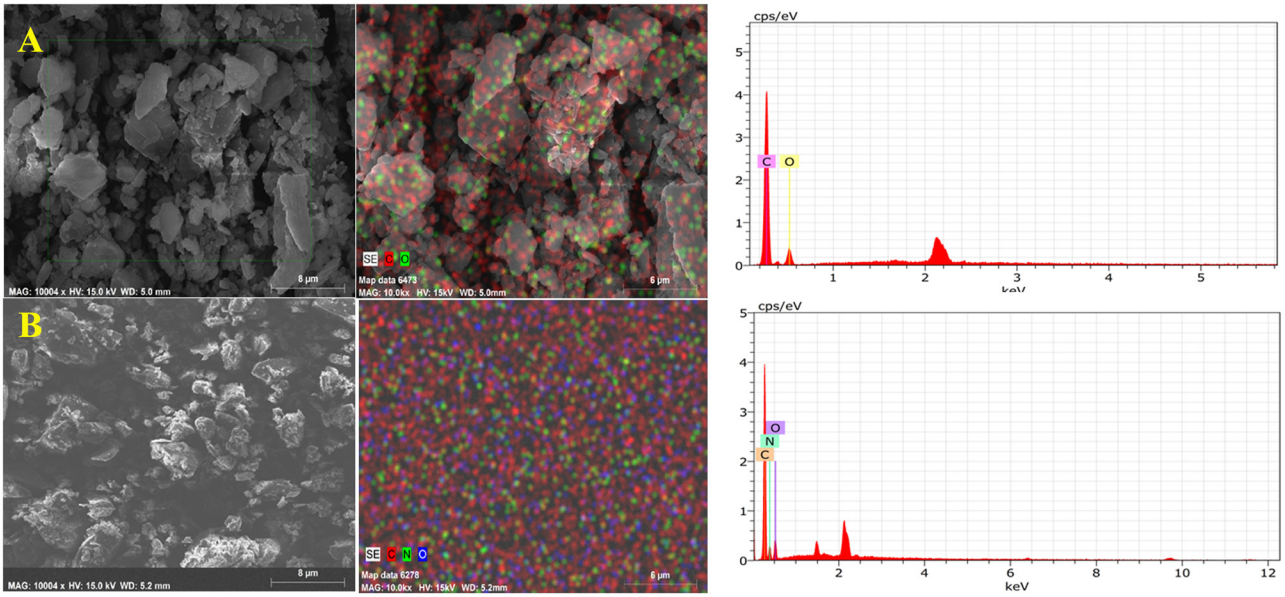

Fig. 7 SEM and EDS photographs along with the elemental analysis profiles of (A) CHRY and (B) the CHRY–THEO (1 : 2) eutectic mixture.

of CHRY and CHRY–THEO (1 : 2), revealing their elemental composition. The EDS spectrum of CHRY showed distinctive peaks for carbon (C) and oxygen (O). Similarly, the EDS spectrum of CHRY–THEO (1 : 2) showed distinctive peaks for carbon (C), nitrogen (N), and oxygen (O). The presence of nitrogen atoms in the CHRY–THEO (1 : 2) eutectic mixture confirmed the presence of THEO. Furthermore, the absence of any other elements in the EDS spectrum of CHRY–THEO (1 : 2) ascertained the purity of the sample.

The morphology of APIs and/or excipients have a remarkable impact on the pharmaceutical performance of the formulations prepared thereof. Thus, SEM was performed to assess the morphological changes brought about in CHRY upon its transformation into the eutectic due to the addition of THEO. Fig. 7 shows the SEM photographs of CHRY and CHRY–THEO (1 : 2). CHRY showed rod/blade shaped crystals while the CHRY–THEO (1 : 2) eutectic displayed a polyhedral shape. The molecular interaction between CHRY and THEO along with the mechanical energy used during the formulation of the eutectic might have changed the morphological characteristics of the prepared eutectic mixture. Furthermore, particle texture, shape, surface morphology, and convexity also have a direct impact on the flowability, mechanical properties like tabletability, compression and compaction, and drug solubility. The morphological characteristics like circularity, convexity, texture, and sphericity of CHRY and CHRY–THEO (1 : 2) were quantitatively analysed. Circularity is a dimensionless parameter that measures how closely a particle appears like a complete circle. It generally decreases during the dry grinding process due to particle size reduction. The circularity of CHRY was found to be 64.26% while that of CHRY–THEO (1 : 2) was found to be 88.04%. Furthermore, convexity represents smoothness and regularity of the particle outer boundary. CHRY displayed a convexity of 79.9% while CHRY–THEO (1 : 2) showed 97.2% convexity. Additionally, the texture of CHRY was 28.76% while that of CHRY–THEO (1 : 2) was observed to be 35.24%. Moreover, the sphericity of CHRY was 64.26% while CHRY–THEO (1 : 2) displayed 88.04% sphericity. Thus, the prepared eutectic mixture demonstrated higher circularity and sphericity as compared to CHRY, suggesting improvement in flow properties due to the reduction in interparticle friction and mechanical interlocking. Furthermore, the enhanced convexity of the eutectic mixture also supported the findings of improvement in flow properties by minimizing surface irregularities. Moreover, improved circularity and sphericity also enhance compressibility, as more regular particles pack efficiently, reducing void spaces and increasing the tablet strength. It is reported that the higher sphericity and smoother texture of CHRY–THEO (1 : 2) *versus* CHRY may promote uniform wetting and reduce agglomeration, leading to faster and more complete dissolution.[27,28]

3.7 Saturation solubility study

As stated earlier, CHRY belongs to BCS II and it is well known that the aqueous solubility of BCS class II drugs limits their oral bioavailability. Thus, to investigate the impact on the aqueous solubility of CHRY upon its formulation into a eutectic mixture, saturation solubility studies were performed. Table 2 presents the saturation solubility of CHRY and CHRY–THEO (1 : 2) in different solvents such as pH 1.2 buffer, pH 6.8 buffer and water at 37 ± 0.5 °C. The CHRY–THEO (1 : 2) eutectic mixture showed significant enhancements of 1.3-fold (water), 2.09-fold (pH 1.2 buffer) and 4.59-fold (pH 6.8 phosphate buffer) in the solubility of CHRY. Such an enhancement in aqueous solubility of CHRY upon its transformation into a eutectic mixture could be associated with the formation of

Table 2 Saturation solubility of CHRY and the CHRY–THEO (1 : 2) eutectic mixture in different solvents

Sample	Distilled water (μg ml^{-1})	0.1 N HCl (pH 1.2) (μg ml^{-1})	Phosphate buffer (pH 6.8) (μg ml^{-1})
CHRY	330.33 ± 1.5275	761.67 ± 2.0817	1261.3 ± 2.30
CHRY : THEO (1 : 2) EM	430 ± 2** (1.30-fold)	1591.3 ± 2.3094*** (2.09-fold)	5790.3 ± 3.0551*** (4.59-fold)

N = 3, data were analysed using one way ANOVA followed by *post hoc* Dunnett's test, with $p < 0.05$ considered significant. *$p < 0.05$ *vs.* control group, **$p < 0.01$ *vs.* control group, ***$p < 0.001$ *vs.* control group.

hydrogen bonds as reflected by FTIR and the increase in the entropy of the system due to mixing which might have disturbed the regular crystal lattice of CHRY.[17,29]

3.8 *In vitro* dissolution studies

The *in vitro* dissolution profiles of CHRY and CHRY–THEO (1 : 2) were recorded using USP type IV apparatus (Fig. 8). CHRY alone showed cumulative 11.5% release over a period of 6 h. However, the prepared eutectic showed 96.20% of CHRY release in a similar time duration, with 90% CHRY released within the initial 2 h. CHRY is a weak acid (pK_a 6.5) and thus exhibits low aqueous solubility owing to its existence in a unionized form at acidic pH. However, in the present work, CHRY showed significant enhancement in aqueous solubility at acidic pH 6.8. This could be associated with the fact that THEO, a weak acid with a pK_a value of 8.8, might have provided a localized buffering effect in the prepared eutectic mixture to maintain a slightly acidic to neutral microenvironment, promoting partial deprotonation of CHRY and also preventing the precipitation of the ionic species of CHRY in GI fluids. Additionally, the significant ($p < 0.05$) improvement in the dissolution rate of CHRY upon formulating into the eutectic mixture could be attributed to the increase in entropy due to mixing and the formation of hydrogen bonds with the coformer THEO which might have altered the crystal lattice of CHRY. Yet, other reasons for dissolution rate enhancement in the case of the CHRY–THEO (1 : 2) mixture are its higher sphericity and smoother texture when compared to CHRY alone, which promoted wetting and reduced agglomeration.

3.9 *In vivo* pharmacokinetic study

The plasma samples showed linearity within a concentration range of 0.5–10 μg ml^{-1}, with an R^2 value of 0.9993 for the bioanalytical method used in the study. The retention times for CHRY and cinnamic acid (IS) were found to be about 6.5 min and 4 min, respectively (Fig. 9). Moreover, the LLOQ and ULOQ of the bioanalytical method were found to be 1 μg ml^{-1} and 10 μg ml^{-1}, respectively, with an accuracy of 0.34%, suggesting minimal chances of systematic error in the analysis. Furthermore, the reproducibility of the method was measured in terms of precision, which was found to be in the range of ±1–4% for individual deviations, suggesting good run-to-run consistency.

The plasma concentration–time profiles of CHRY alone and the CHRY–THEO (1 : 2) formulation after oral administration of a single dose to fasting male Wistar rats are shown in Fig. 10. The pharmacokinetic parameters extracted from the profiles are presented in Table 3. The C_{max} of CHRY was found to be significantly increased by 3.60-fold when formulated into the eutectic mixture. Moreover, approximately 3-fold increases in $AUC_{(0-24)}$ and $AUC_{(0-\infty)}$ of CHRY were seen upon its transformation into the eutectic mixture with THEO. Additionally, the relative bioavailability (F_{rel}) of CHRY–THEO (1 : 2) was 2.87-fold higher than that of CHRY alone. Thus, the findings of the *in vivo* studies were in accordance with the *in vitro* dissolution profiles, suggesting an improvement in the oral bioavailability of CHRY. The significant increase in the aqueous solubility of BCS class II CHRY could be attributed to its enhancement in bioavailability. THEO, a BCS class I molecule, has been reported to show 96% oral biovailability.[30,31] THEO was con-

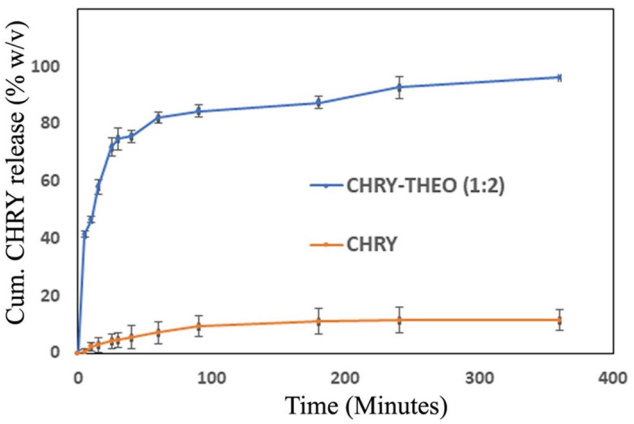

Fig. 8 Dissolution profiles of CHRY and the CHRY–THEO (1 : 2) eutectic mixture in phosphate buffer pH 6.8 using flow through cell apparatus.

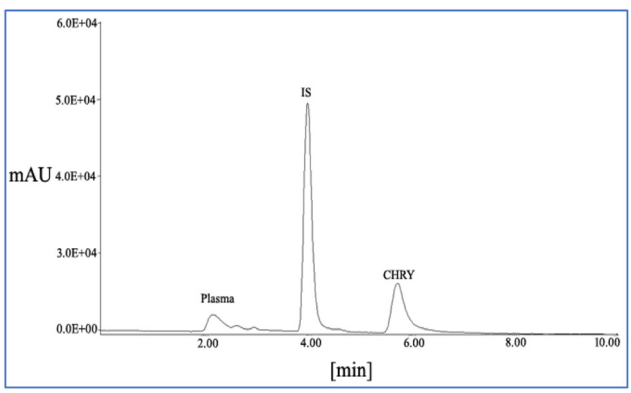

Fig. 9 Representative chromatogram of CHRY and cinnamic acid (IS) spiked in rat plasma.

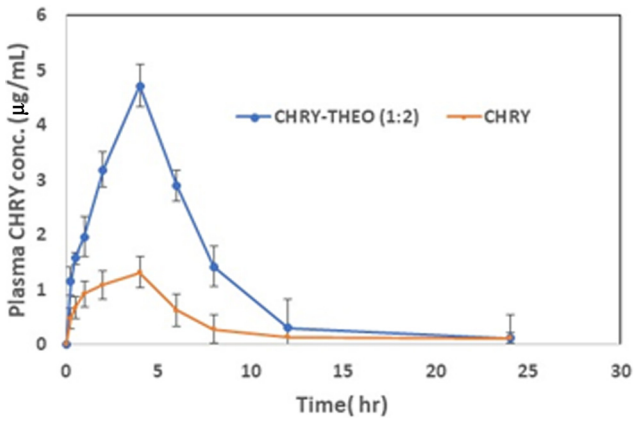

Fig. 10 Plasma CHRY profiles of CHRY alone and the CHRY–THEO (1 : 2) eutectic mixture upon administration of a single oral dose in Wister rats (N = 6).

Table 3 Pharmacokinetic parameters of CHRY after oral gavage administration to rats

Pharmacokinetic parameters	CHRY	CHRY–THEO (1 : 2)
C_{max} (µg mL^{-1})	1.31 ± 1.29	4.72 ± 0.37***
T_{max} (h)	4	4
AUC_{0-t} (h µg mL^{-1})	10.62 ± 2.06	30.51 ± 2.61***
$t_{1/2}$ (h)	3.82 ± 0.39	6.67 ± 1.04***
Cl (mL min^{-1})	0.23 ± 0.07	0.081 ± 0.004***
F_{rel}	—	2.87

Mean ± SEM, n = 6. Data were analyzed using ANOVA followed by *post hoc* Dunnett's test. Statistical significance compared with CHRY. ***P < 0.001, **P < 0.05.

sidered as a coformer in the present study and owing to the fact that it belongs to BCS class I, we did not measure the plasma THEO levels. THEO exhibits a narrow therapeutic index and is metabolized *via* CYP1A2[30,31], limiting its clinical use. In the present work, we successfully increased the bioavailability of CHRY, which is known to inhibit CYP1A2[8] and also show anti-inflammatory activity by inhibiting key pro-inflammatory cytokines such as TNF-α, IL-1β, IL-6, IL-12, and IL-17A, and by downregulating nuclear transcription factor NF-κB, a central regulator of inflammatory responses.[32–34] Thus, the prepared eutectic mixture is expected to play dual roles of reducing the dose of THEO due to the inhibition of CYP1A2 and exhibiting synergistic anti-inflammatory activity which could be fruitful in the management of COPD and asthma.

Although the present study showed remarkable improvements in the aqueous solubility and in turn the bioavailability of CHRY, the risk associated with elevated THEO plasma concentrations cannot be overlooked. The inhibition of CYP1A2 enzymes by CHRY may increase the plasma THEO concentrations above the therapeutic level due to its narrow therapeutic index, which may show adverse effects such as nausea, vomiting, tachycardia, arrhythmias, seizures, and central nervous system toxicity. Thus, the current formulation would require therapeutic drug monitoring (TDM) before it is advanced toward clinical use. Moreover, the current work needs further clinical evaluation to assess its suitability in the management of COPD and asthma.

5. Conclusion

In conclusion, a eutectic mixture of chrysin was successfully formulated with theophylline using a simple, cost-effective, green dry grinding method in a stoichiometric ratio of 1 : 2 respectively. The prepared mixture was characterized using DSC, FTIR, HSM, TGA, EDS, *in vitro* dissolution studies and *in vivo* pharmacokinetic studies in Wistar rats. The mixture demonstrated significant enhancements in saturation solubility, dissolution rate and in turn oral bioavailability of chrysin. Furthermore, the prepared mixture is believed to play dual roles in the treatment of COPD and asthma as chrysin and theophylline together will show anti-inflammatory activity along with improvement in the bioavailability of theophylline due to the inhibition of cytochrome enzymes responsible for degradation of theophylline by chrysin, for which further clinical evaluations are needed. The present work demonstrates a simple, economical method for the possible treatment of COPD and asthma.

Conflicts of interest

The authors report no conflict of interest.

Ethics approval and consent to participate

The animal experimentation procedures were followed in accordance with CPCSEA guidelines.

Data availability

The datasets generated during and/or analysed during the current study are available from the corresponding author on reasonable request.

Acknowledgements

The authors gratefully acknowledge the financial support from the Department of Science and Technology (DST) through the Fund for Improvement of S&T Infrastructure in Universities and Other Higher Educational Institutions (FIST) program (File No: SR/FST/COLLEGE-/2019/526).

References

1 S. Momtazmanesh, S. S. Moghaddam, S.-H. Ghamari, *et al.*, Global Burden of Chronic Respiratory Diseases and Risk Factors, 1990–2019: An Update from the Global Burden of Disease Study 2019, *eClinicalMedicine*, 2023, **59**, 101936, DOI: 10.1016/j.eclinm.2023.101936.

2 S. Safiri, K. Carson-Chahhoud, M. Noori, S. A. Nejadghaderi, M. J. M. Sullman, J. Ahmadian Heris, K. Ansarin, M. A. Mansournia, G. S. Collins, A.-A. Kolahi and J. S. Kaufman, Burden of Chronic Obstructive Pulmonary Disease and Its Attributable Risk Factors in 204 Countries and Territories, 1990–2019: Results from the Global Burden of Disease Study 2019, *Br. Med. J.*, 2022, **378**, e069679, DOI: 10.1136/bmj-2021-069679.

3 J. Szarłowicz, M. Mazur, D. Waz, Z. Goliszek, K.Ł Sobek, W. Tabin-Barczak, A. Sokołowska, K. Fikas, K. Chwaliszewski and S. Samuła, Theophylline Revisited. Mechanisms, Challenges, and New Horizons, *Qual. Sport*, 2025, **37**, 57009, DOI: 10.12775/qs.2025.37.57009.

4 P. Barnes and R. Pauwels, Theophylline in the Management of Asthma: Time for Reappraisal?, *Eur. Respir. J.*, 1994, **7**(3), 579–591, DOI: 10.1183/09031936.94.07030579.

5 P. J. Barnes, Theophylline, *Pharmaceuticals*, 2010, **3**(3), 725–747, DOI: 10.3390/ph3030725.

6 N. Gresa-Arribas, J. Serratosa, J. Saura and C. Solà, Inhibition of CCAAT/Enhancer Binding Protein δ Expression by Chrysin in Microglial Cells Results in Anti-Inflammatory and Neuroprotective Effects, *J. Neurochem.*, 2010, **115**(2), 526–536, DOI: 10.1111/j.1471-4159.2010.06952.x.

7 D. Baidya, J. Kushwaha, K. Mahadik and S. Patil, Chrysin-Loaded Folate Conjugated PF127-F68 Mixed Micelles with Enhanced Oral Bioavailability and Anticancer Activity against Human Breast Cancer Cells, *Drug Dev. Ind. Pharm.*, 2019, **45**(5), 852–860, DOI: 10.1080/03639045.2019.1576726.

8 J. Yao, M. Jiang, Y. Zhang, X. Liu, Q. Du and G. Feng, Chrysin Alleviates Allergic Inflammation and Airway Remodeling in a Murine Model of Chronic Asthma, *Int. Immunopharmacol.*, 2016, **32**, 24–31, DOI: 10.1016/j.intimp.2016.01.005.

9 G. C. Bazzo, B. R. Pezzini and H. K. Stulzer, Eutectic Mixtures as an Approach to Enhance Solubility, Dissolution Rate and Oral Bioavailability of Poorly Water-Soluble Drugs, *Int. J. Pharm.*, 2020, **588**, 119741, DOI: 10.1016/j.ijpharm.2020.119741.

10 C. F. Wahlgren and H. Quiding, Depth of Cutaneous Analgesia after Application of a Eutectic Mixture of the Local Anesthetics Lidocaine and Prilocaine (EMLA Cream), *J. Am. Acad. Dermatol.*, 2000, **42**(4), 584–588.

11 C. S. Yong, Y.-K. Oh, S. H. Jung, J.-D. Rhee, H.-D. Kim, C.-K. Kim and H.-G. Choi, Preparation of Ibuprofen-Loaded Liquid Suppository Using Eutectic Mixture System with Menthol, *Eur. J. Pharm. Sci.*, 2004, **23**(4–5), 347–353, DOI: 10.1016/j.ejps.2004.08.008.

12 D. R. Serrano, T. Persoons, D. M. D'Arcy, C. Galiana, M. A. Dea-Ayuela and A. M. Healy, Modelling and Shadowgraph Imaging of Cocrystal Dissolution and Assessment of in Vitro Antimicrobial Activity for Sulfadimidine/4-Aminosalicylic Acid Cocrystals, *Eur. J. Pharm. Sci.*, 2016, **89**, 125–136, DOI: 10.1016/j.ejps.2016.04.030.

13 L. Meneses, F. Santos, A. Gameiro, A. Paiva and A. Duarte, Preparation of Binary and Ternary Deep Eutectic Systems, *J. Visualized Exp.*, 2019, **152**, e60326, DOI: 10.3791/60326.

14 I. Qader, M. Laguerre, A. Lavaud, M. Tenon, K. Prasad and A. Abbott, Selective Extraction of Antioxidants by Formation of a Deep Eutectic Mixture through Mechanical Mixing, *ACS Sustainable Chem. Eng.*, 2023, **11**(10), 4168–4176, DOI: 10.1021/acssuschemeng.2c06894.

15 A. Baclig, D. Ganapathi, V. Ng, E. Penn, J. Saathoff and W. Chueh, Large Decrease in the Melting Point of Benzoquinones via High-n Eutectic Mixing Predicted by a Regular Solution Model, *J. Phys. Chem. B*, 2023, **127**(27), 6102–6112, DOI: 10.1021/acs.jpcb.3c01125.

16 B. Hansen, S. Spittle, B. Chen, D. Poe, Y. Zhang, J. Klein, A. Horton, L. Adhikari, T. Zelovich, B. Doherty, B. Gurkan, E. Maginn, A. Ragauskas, M. Dadmun, T. Zawodzinski, G. Baker, M. Tuckerman, R. Savinell and J. Sangoro, Deep Eutectic Solvents: A Review of Fundamentals and Applications, *Chem. Rev.*, 2020, **121**(3), 1232–1285, DOI: 10.1021/acs.chemrev.0c00385.

17 S. Di Muzio, F. Trequattrini, O. Palumbo, P. Roy, J. Brubach and A. Paolone, An Eutectic Mixture in the Tetrabutylammonium Bromide-Octanol System: Macroscopic and Microscopic Points of View, *ChemPhysChem*, 2024, **25**(16), e202400219, DOI: 10.1002/cphc.202400219.

18 X. Hou, L. Yu, C.-H. He and K.-J. Wu, Group and Group-Interaction Contribution Method for Estimating the Melting Temperatures of Deep Eutectic Solvents, *AIChE J.*, 2021, **68**(2), e17408, DOI: 10.1002/AIC.17408.

19 J. Lane, V. Klimkowski and T. Hopkins, Molecular Dynamics Investigation of Deep Eutectic Solvent Structure and Properties Based on Hydrogen Bond Acceptor Variation, *J. Mol. Liq.*, 2025, **423**, 127009, DOI: 10.1016/j.molliq.2025.127009.

20 M. Dzhavakhyan and Y. Prozhogina, Deep Eutectic Solvents: History, Properties, and Prospects, *Pharm. Chem. J.*, 2023, **57**, 296–299, DOI: 10.1007/s11094-023-02879-0.

21 M. Talebi, M. Talebi, T. Farkhondeh, J. Simal-Gándara, D. Kopustinskiene, J. Bernatonienė and S. Samarghandian, Emerging Cellular and Molecular Mechanisms Underlying Anticancer Indications of Chrysin, *Cancer Cell Int.*, 2021, **21**, 214, DOI: 10.1186/s12935-021-01906-y.

22 P. Ittadwar and P. Puranik, Analytical Method Development, Characterization, Evaluation of *In vitro* Antioxidant and Anticancer Activity of Flavone Chrysin in HeLa Cells, *Int. J. Pharm. Sci. Drug Res.*, 2020, **13**(5), 457–469, DOI: 10.25004/ijpsdr.2021.130502.

23 A. Okunlola and S. A. Adewusi, Development of Theophylline Microbeads Using Pregelatinized Breadfruit Starch (Artocarpus Altilis) as a Novel Co-Polymer for Controlled Release, *Adv. Pharm. Bull.*, 2019, **9**, 93–101, DOI: 10.15171/apb.2019.012.

24 A. Wynne, B. Abbott, R. Niazi, K. Foley and K. Walters, Experimental and Modeling Approaches to Determine Drug Diffusion Coefficients in Artificial Mucus, *Heliyon*, 2024, **10**(20), e38638, DOI: 10.1016/j.heliyon.2024.e38638.

25 R. Chadha, Y. Bhalla, A. Nandan, K. Chadha and M. Karan, Chrysin Cocrystals: Characterization and Evaluation, *J. Pharm. Biomed. Anal.*, 2017, **134**, 361, DOI: 10.1016/j.jpba.2016.10.020.

26 S. Ren, F. Nian, X. Chen, R. Xue and F. Chen, Routes of Theophylline Monohydrate Dehydration Process Proposed by Mid-Frequency Raman Difference Spectra, *J. Pharm. Sci.*, 2023, **112**(11), 2863–2868, DOI: 10.1016/j.xphs.2023.06.005.

27 J. Rivera, C. Pelosi, E. Pulidori, C. Duce, M. Tiné, G. Ciancaleoni and L. Bernazzani, Guidelines for a Correct Evaluation of Deep Eutectic Solvents Thermal Stability, *Curr. Res. Green Sustainable Chem.*, 2022, **5**, 100333, DOI: 10.1016/j.crgsc.2022.100333.

28 N. Delgado-Mellado, M. Larriba, P. Navarro, V. Rigual, M. Ayuso, J. García and F. Rodríguez, Thermal Stability of Choline Chloride Deep Eutectic Solvents by TGA/FTIR-ATR Analysis, *J. Mol. Liq.*, 2018, **260**, 37–43, DOI: 10.1016/J.MOLLIQ.2018.03.076.

29 E. Crespo, L. Silva, M. Martins, M. Bülow, O. Ferreira, G. Sadowski, C. Held, S. Pinho and J. Coutinho, The Role of Polyfunctionality in the Formation of [Ch]Cl-Carboxylic Acid-Based Deep Eutectic Solvents, *Ind. Eng. Chem. Res.*, 2018, **57**(32), 11195–11209, DOI: 10.1021/ACS.IECR.8B01249.

30 L. Hendeles, M. Weinberger and L. Bighley, Absolute Bioavailability of Oral Theophylline, *Am. J. Hosp. Pharm.*, 1977, **34**(5), 525–527, DOI: 10.1093/AJHP/34.5.525.

31 J. Jonkman, W. Berg, R. Schoenmaker, J. Greving, R. Dezeeuw and N. Orie, Absolute bioavailability of microcrystalline theophylline, *Curr. Med. Res. Opin.*, 1979, **6**, 71–76, DOI: 10.1185/03007997909115912.

32 X. Feng, H. Qin, Q. Shi, Y. Zhang, F. Zhou, H. Wu, S. Ding, Z. Niu, Y. Lu and P. Shen, Chrysin Attenuates Inflammation by Regulating M1/M2 Status via Activating PPARγ, *Biochem. Pharmacol.*, 2014, **89**(4), 503–514, DOI: 10.1016/j.bcp.2014.03.016.

33 T. Liao, L. Ding, P. Wu, L. Zhang, X. Li, B. Xu, H. Zhang, Z. Ma, Y. Xiao and P. Wang, Chrysin Attenuates the NLRP3 Inflammasome Cascade to Reduce Synovitis and Pain in KOA Rats, *Drug Des., Dev. Ther.*, 2020, **14**, 3015–3027, DOI: 10.2147/DDDT.S261216.

34 M. Zeinali, S. Rezaee and H. Hosseinzadeh, An Overview on Immunoregulatory and Anti-Inflammatory Properties of Chrysin and Flavonoids Substances, *Biomed. Pharmacother.*, 2017, **92**, 998–1009, DOI: 10.1016/j.biopha.2017.06.003.